ORIGINAL PAPER

Residual-state creep behavior of typical clayey soils

Deepak R. Bhat · N. P. Bhandary · R. Yatabe

Abstract Few researchers have studied the creeping displacement behavior of clayey soils using a triaxial compression cell and oedometer; however, in most cases, they have concentrated on the pre-peak state of shear. Clayey soil from a landslide is assumed to have already reached the residual-state, necessitating a study on residual strength to understand the creeping displacement behavior of clayey soils from landslides. In this work, an existing torsional ring shear apparatus was modified to understand the creeping displacement behaviors of typical clayey soil. The newly developed creep test apparatus is capable of measuring the displacement with respect to time under the application of a constant creep stress. This paper focuses mainly on residual-state creep behaviors of typical clayey soils. Residual-state creep failure prediction curves are also proposed, which may be used to predict failure time and displacement of creeping landslides in the future.

Keywords Clayey soils · Modified torsional ring shear apparatus · Residual-state creep test · Creeping displacement behavior

1 Introduction

The shearing strength of a soil sample is defined generally as its maximum resistance to shearing forces (Skempton 1964a, b, 1985; Bishop et al. 1971; Lupini et al. 1981; Gibo and Egashira 1992; Gibo 1994; Nakamura et al. 2010). The shearing strength of a soil is described in terms of peak strength and residual strength. When a soil sample has sheared, the shear stress normally reaches a peak value at a small shear displacement called the peak strength. When the shear displacement increases to a large value, it undergoes post-peak strength loss until a constant minimum value is reached. This is called residual strength (Skempton 1964a, b, 1985; Lupini et al. 1981). In his Rankine Lecture (1964b), Skempton

D. R. Bhat (✉) · N. P. Bhandary · R. Yatabe
Geo-Disaster Research Laboratory, Graduate School of Science and Engineering,
Ehime University, 3 Bunkyo, Matsuyama 790-8577, Japan
e-mail: deepakrajbhat@gmail.com

highlighted the concept of the residual shear strength of soils, drawing attention to its nature and its engineering significance. Skempton (1964a, b) suggested that the drained residual strength is mobilized along pre-existing shear surfaces caused by previous landslides and tectonic shearing. Skempton (1964a, b, 1985) demonstrated that the post-peak drop in drained strength of an intact overconsolidated clay might take place in two stages. First, at a relatively small displacement, the strength decreases to the "fully softened" or "critical state" value, as the water content of the clay increases (dilatancy); and second, the shearing resistance drops from the fully softened to the residual condition owing to the orientation of plate-shaped particles along the shear plane. The post-peak drop in strength of normally consolidated clay is due entirely to particle reorientation (Skempton and Petley 1967; Morgenstern and Tchalenko 1967; Lupini et al. 1981).

In the laboratory, the reversal direct shear test and torsional ring shear test are used to measure the residual shear strength of soil specimens (Bishop et al. 1971; Chandler 1977; Bromhead and Dixon 1986; Stark and Eid 1994). Triaxial testing is the most commonly used test to measure the shear strength of soils; however, the main drawback of the triaxial device is limited available shear displacement (Bishop et al. 1971, Sassa 1992). The use of a triaxial test to measure residual shear strength is not preferred (Skempton and Petley 1967). The reversal direct shear test is used widely to measure the residual strength of soils even though it has several limitations (Stark and Eid 1994; Wan and Kwong 2002; Meehan et al. 2010). The primary limitation is that it can only shear the specimen in the forward and backward direction until a minimum shear resistance is measured. Each reversal of the shear box results in a horizontal displacement of <0.5 cm (Stark and Eid 1994). As a result, the specimen is not subjected to continuous shear to large deformation in one direction, and thus, a full orientation of the clay particles parallel to the direction of shear may not be obtained. Hence, the residual value measured by the reversal direct shear may not be accurately simulating the field conditions in which large relative displacement occurs without change in direction (Skempton 1985, Stark and Eid 1994).

More recently days, a torsional ring shear apparatus has been widely used to obtain the residual shear strength of a soil. The main advantage of the torsional ring shear apparatus is that it can shear the specimen continuously in one direction to obtain the large displacement, and this allows clay particles to be oriented parallel to the direction of shear to develop the true residual shear strength condition (La Gatta 1970; Bishop et al. 1971; Bromhead 1979; Tika 1999; Suzuki et al. 2007). Another advantage of ring shear apparatus is that no change occurs in the shear plane area during shearing. For the precise measurement of residual strength, the large deformation is applied to a specimen so that platy clay minerals are oriented parallel to the shear plane (Skempton 1985, Gibo 1994). For that objective, the ring shear apparatus has been used frequently.

Skempton (1970) affirmed the use of the residual strength in the analysis of reactivated landslides in stiff fissured clays. Skempton (1985) mentioned that the field residual strength value for the slip surface soil of a landslide should be the same as the strength calculated from the back analysis of the landslide, in which movement has reactivated along a pre-existing slip surface. It means the back analyzed and laboratory determined strength parameters must be the same such that the laboratory tests are carried out in precise in situ conditions. Bromhead and Curtis (1983), Mesri and Feng (1986), Stark and Eid (1994), Tika and Hutchinson (1999), Mesri and Shahien (2003), Stark et al. (2005), and Tiwari and Marui (2005) concluded that the drained residual shear strength measured in a ring shear apparatus is in agreement with the back-calculated drained residual shear strength for landslide slip surface. This shows the importance of residual shear strength in understanding the creeping displacement behavior of slip surface clayey soil from a creeping

landslide. If a creep testing apparatus can facilitate the direct application of creep stress on the residual-state of shear and measure its displacement with respect to time, the test results would be useful in understanding the creep displacement behavior of clayey soils from a landslide.

Different approaches to explain soil creep in natural slopes have been reported (Ter-Stepanian 1963, 1975; Yen 1969; Nelson and Thompson 1977). Terzaghi (1950), however, was most likely the first to consider the relationship between soil creep and landslides. Ter-Stepanian (1963) introduced the threshold approach to explain soil creep in simple natural slopes by considering the zone of creep and its rate as being dependent on the groundwater level. The effective stress state of the sample shifts with time toward the failure envelope for the clay during creep (Waker 1969). A theory of creep failure was meant to explain the phenomenon of creep, strain softening, and time-dependent failure in overconsolidated clay under considering the triaxial test and field observation results (Nelson and Thompson 1977). Patton (1984) discussed the creep displacement of the landslide as directly related to the groundwater condition. Suklje (1969) and Leroueil et al. (1985) described the behavior of the soil, which becomes dependent on the current stress and strain rate and is independent of the past history; however, the time-dependent deformation phenomenon is more pronounced in clayey soils. The creep of soil has been interpreted by rate process theory using experimental data from four types of soils (Feda 1989). The time-dependent behavior of clay soil and sand has been investigated through one-dimensional and triaxial test conditions. It was concluded that time-dependent phenomenon is more pronounced in clay than sand (Augustesen et al. 2004). Picarelli et al. (2004) studied the creep behavior in brittle soils in which the strength decreases drastically from the peak value to the residual value; hence, the first-time slide velocity is quite high. After failure, the landslide progressively slows down as long as the strength approaches the residual value. Picarelli et al. (2004) showed that reactivation involves old landslide bodies, or part of them, sliding along the existing slip surface when the induced shear stress exceeds the residual value. Long-term investigation and monitoring of deep-seated creeping landslide in southern swiss has been done to better understand the factor controlling the landslide movement (Eberhardt st al. 2007a, b). Leoni et al. (2008) presented a new anisotropic model for the time-dependent behavior of soft soil using triaxial compression test data. The responses under the constant stress condition of volcanic clayey soils discussed were based on triaxial test results (Brandes and Nakayama 2010). A modeling method intended to understand the viscous behavior of soft clay on constant strain-rate oedometer test and 24-h standard oedometer test (Yin et al. 2010).

Few researches (Ter-Stepanian 1963; Yen 1969; Waker 1969; Campanella et al. 1974; Nelson and Thompson 1977; Patton 1984; Feda 1989; Picarelli et al. 2001; Picarelli et al. 2004; Augustesen et al. 2004; Bonzanigo et al. 2007a, b; Leoni et al. 2008; Yin et al. 2010; Brandes and Nakayama 2010, etc.) have studied the creeping displacement behavior of clayey soils using both a triaxial testing apparatus and oedometer; however, in most cases, they have only concentrated on the pre-peak state of shear (i.e., up to peak strength). In the pre-peak state of shear, a soil material is in the process of losing or has already lost the effect of cohesion and adhesion, and interlocking and dilatancy, and the minimum strength after undergoing a large displacement depends upon the internal friction between the soil particles. That means landslide soils may not show the creeping displacement behaviors in the pre-peak state because these soils have already reached the post-peak state, especially in the residual-state (Bhat et al. 2011d). If a creep test can be performed on the residual-state of shear, creeping mechanisms and the displacement behavior of landslides may be understood. Bhat et al. (2011c, 2012a) purposed a new concept of the residual-state creep

test using a modified torsional ring shear apparatus to understand the creeping displacement behavior of clayey soils from landslides. The prediction curves are purposed based on residual-state creep test results, which may be used to predict the failure time and displacement of creeping landslides (Bhat et al. 2011a, b). The role of clay minerals for landslide reactivation and creeping displacement behavior of clayey soils having higher percentage of smectite, chlorite, and mica are discussed (Bhat et al. 2012b). In this work, an attempt has been made to measure residual-state creep. For this purpose, a residual-state creep test apparatus is developed. The main objective of this study is to understand the residual-state creep behavior of clayey soils.

2 Materials and method

Clayey soils from the slip surface of landslides normally include the presence of clay minerals such as smectite, chlorite, and mica or illites. Such minerals have very high specific surface, cation exchange capacity, and affinity to water, which makes them swell significantly. Swelling of such mineral particles significantly reduces the strength of soil. It is therefore considered that clayey soils influence the creeping displacement behavior of landslides (Yatabe et al. 1991, 2007; Tori and Kitagawa 2006). In this study, four typical clayey soils were taken. One sample was commercially available kaolin clay, and the three clayey soils were collected from the creeping landslide sites in Japan and Nepal. Soil samples from the Shikoku landslide area of Japan were conformed to have a comparatively high amount of chlorite and were called a "chlorite-rich sample." The soil sample from Kobe the landslide area of Japan was conformed to have a comparatively high amount of smectite and was called a "smectite-rich sample." Similarly, the sample from the Krishnabhir landslide area in Nepal was conformed to have a comparatively high amount of mica and was called a "mica-rich sample." A summary of the major minerals determined by the X-ray diffraction test is shown in Table 1.

Table 2 shows the physical properties of typical clayey soils. The solid density of the mica-rich sample and chlorite-rich sample is higher than the solid density of kaolin clay is (Table 2). Similarly, the solid density of the smectite-rich sample is lower than the solid density of kaolin clay is. The plasticity index of kaolin clay is lower than the smectite-rich sample and higher than the mica-rich sample and the chlorite-rich sample. The clay particles (i.e., <2 μm) of the kaolin clay are the highest and the smectite-rich sample, mica-rich sample, and chlorite-rich sample follow it, respectively (Table 2). Figure 1 shows the grain size distribution curves.

Torsional ring shear apparatus based on the concept reported by Bishop et al. (1971) was used in this study. In this apparatus, the specimen container has inner and outer

Table 1 Major minerals, determined by X-ray diffraction tests

Sample type	Peak intensity of main constituent minerals (cps)			
	Smectite	Chlorite	Mica	Felspar
Mica-rich sample	–	2,415	3,600	–
Chlorite-rich sample	755	2,090	1,425	1,125
Smectite-rich sample	1,630	–	–	490

Table 2 Physical properties of tested samples

Sample type	Solid density (g/cm³)	Liquid limit (%)	Plastic limit (%)	Plasticity index (%)	Soil classification (%)		
					<2 μm	2–75 μm	75–425 μm
Kaolin clay	2.72	52	22	30	74	26	0
Mica-rich sample	2.74	34	21	13	21	60	19
Chlorite-rich sample	2.75	48	31	17	20	68	12
Smectite-rich sample	2.65	97	59	38	24	55	21
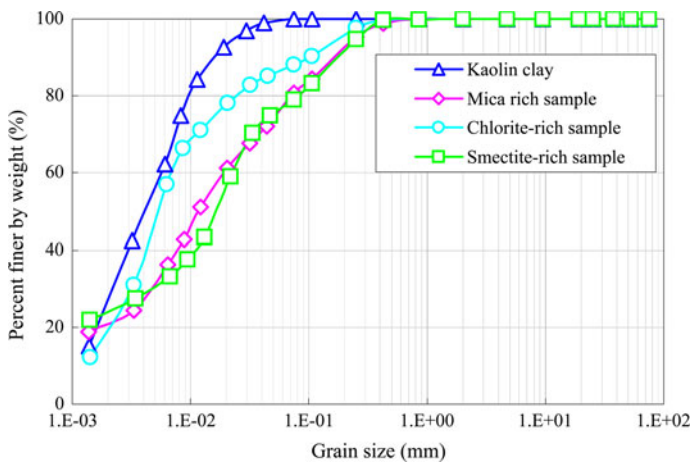
Fig. 1 Grain size distribution curves

diameters of approximately 8.0 and 12.0 cm, respectively, and a depth of 3.2 cm. The ratio of the outer to inner ring diameters is 1.5. To perform the residual-state creep test, the ring shear apparatus was modified based on the transitional change of the strain-controlled motor-driven shear into creep load shearing without completely releasing the applied shear stress, which is capable of measuring the creep displacement with respect to time under the application of a constant creep load, as shown in Fig. 2. The lower part of the ring shear apparatus was developed in such a way that the overall effect of the creep load acts directly on the shearing zone of the test specimen, and the displacement or deformation due to the application of a constant creep load was recorded in the displacement recorder unit. The deformation of the specimen with respect to time and the corresponding changes in the volume of the specimen, if any, during the creep tests is recorded automatically. The shearing of the specimen is performed until the specimen reaches the residual state of shear after a large displacement of shearing; then, the shearing process is stopped and residual-state creep test is begun.

In the residual-state creep test, there are two main steps: (1) the ring shear test and (2) the residual-state creep test. The ring shear test is performed to obtain the residual-state of shear of specimens in the fully saturated state. This state is confirmed when the shearing has reached the residual-state, indicating constant values for the load-cell reading and dial gauge reading after a large displacement; then, the specimen is ready for the residual-state
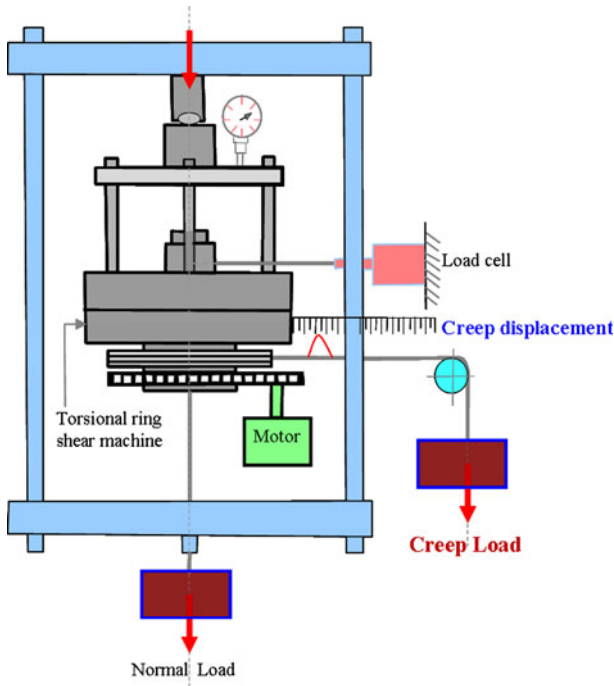
Fig. 2 Modification of the torsional ring shear apparatus

creep test. In the residual-state creep test, the creep load is initially applied at 90 % of its residual-state of shear, which is equivalent to an RCSR of 0.9000. The term RCSR is the ratio of the applied constant creep stress to the residual strength. Then, the specimen is left for several hours in the same condition to determine whether the effect of the creeping displacement behavior is significant or not. Similarly, the creep load is slightly increased in different steps until the specimen reaches failure. The overall experimental flow of the residual-state creep test is shown in Fig. 3.

All samples were prepared by remolding below 425 μm and overconsolidated under a normal pressure of 196.2 kN/m^2. To avoid the extra machine friction, all shear tests were conducted under a normal pressure of 98.1 kN/m^2. The shearing condition was confirmed to be drained by allowing sufficient time to dissipate excess pore water pressure, for which the average rate of displacement through the slip surface was set at 0.16 mm/min. The controlled shearing of the sample was performed until it reached its residual strength after a large displacement. Then, the shearing process was stopped, and the sample was ready for the creep test. In the residual-state creep test, the creep stress applied initially 90 % of the residual-state of shear, which is equivalent to an RCSR of 0.9000. Then, the specimen is left for several hours in the same condition to determine whether the effect of the creep displacement behavior is significant or not. Similarly, the creep load is applied accordingly with RCSR values of 0.9500, 1.000, 1.0025, 1.0050, 1.0100, 1.0125, 1.01500, and 1.0200 until the specimen fails (Fig. 4).

Fig. 3 Overall experimental flow of residual-state creep test
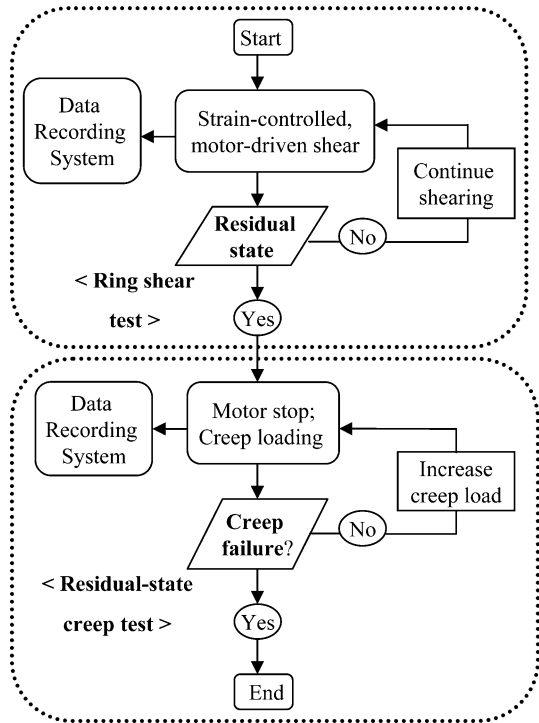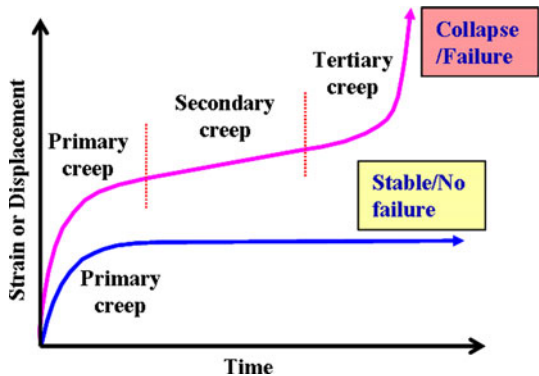

Fig. 4 Ideal creep curve

Some assumptions made in this study are listed below:

1. At the residual state of shear, there is no influence of further displacement on the shear resistance of the slip surface soil.
2. The recovery of the shear resistance due to a reduction in the rate of shear or due to the state of no shear is neglected.
3. The fluctuation of the shear resistance due to sample preparation, effective stress application accuracy, etc., is neglected.
4. The change in the shear behavior due to changes in the value of the RCSR, if any, is neglected.

5. The process of creep has been defined based on ideal creep curve concept as shown in Fig. 4.
    Primary creep (I): decreasing strain rate
    Secondary creep (II): constant strain rate
    Tertiary creep (III): accelerating strain rate, generally to creep rupture or failure

3 Results and discussion

In the residual-state creep test, initially, a ring shear test was performed to obtain the residual-state of shear, then the creep test was begun. Typical ring shear test results on kaolin clay, mica-rich sample, chlorite-rich sample, and smectite-rich sample were presented in terms of variation of shear stress and specimen depth with the shear displacement (Fig. 5). Residual-state of shear in each case was obtained after 10.0 cm of shear displacement except in the smectite-rich sample. For the confirmation of residual-state of shear, the ring shear test of the smectite-rich sample was preceded by up to 20.0 cm of shear displacement and up to 15.0 cm for remaining soil specimens (Fig. 5). Since the sample preparation and test procedures were conducted in certain set procedures, the residual-state of shear of each sample in each test were found to be in close agreement.

Figures 6, 7, 8, and 9 show the typical residual-state creep test on kaolin clay, mica-rich sample, chlorite-rich sample, and smectite-rich sample, respectively. Similarly, six more tests for each sample were conducted with varying applied constant creep load. The results thus obtained were summarized in Tables 3, 4, 5, and 6. In this study, different stages of creep were defined based on the change in displacement (Fig. 4). In primary creep, the change in displacement decreases. When the change in displacement is constant, it is called secondary creep. In tertiary creep, the change in displacement is suddenly increased, which leads to failure. T_1 represents the total time at the end of primary creep (that is beginning of the secondary creep) and its corresponding displacement, D_1. Similarly, T_2 and D_2 represent the total time at the end of secondary creep (i.e., beginning of tertiary creep) and total displacement at time T_2, respectively, as shown in Figs. 6, 7, 8, and 9.

The different stages of creep were defined based on the concept of ideal creep curve (Fig. 4) for a soil material under the application of constant creep stress. The test results for each specimen of each case were found to perfectly match with ideal creep curve concept (Figs. 6, 7, 8, 9). Lefebvre (1981) proposed that creep failure can occur at less than peak
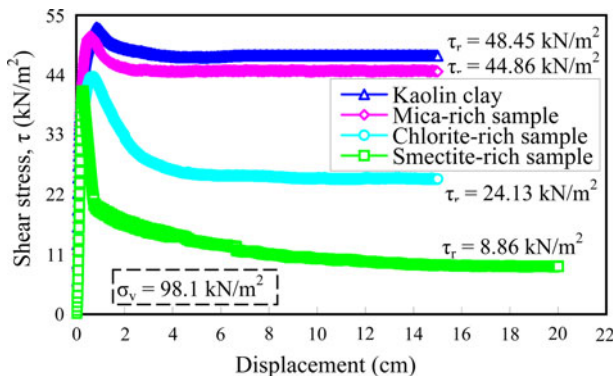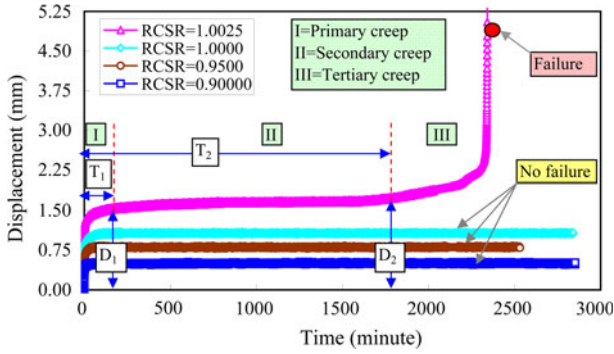

Fig. 5 Typical ring shear tests

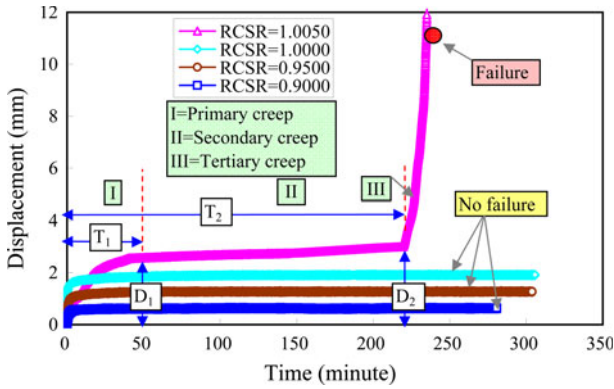**Fig. 6** Typical residual-state creep test on kaolin clay

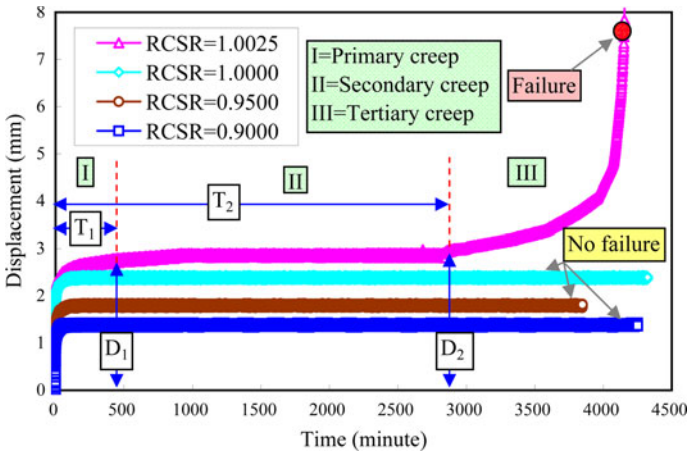**Fig. 7** Typical residual-state creep test on mica-rich sample

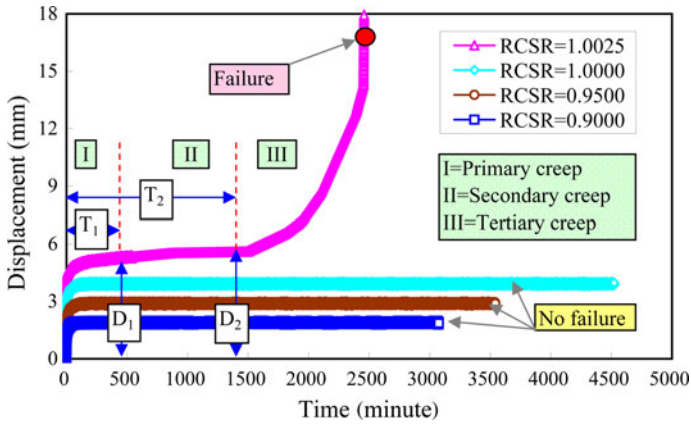**Fig. 8** Typical residual-state creep test on chlorite-rich sample

Fig. 9 Typical residual-state creep test on smectite-rich sample

Table 3 Summary of residual-state creep tests on kaolin clay

Test	RCSR	T_1 (min)	D_1 (mm)	T_2 (min)	D_2 (mm)	Remarks
7	1.0200	0.23	1.42	3.03	0.49	Failure
6	1.0150	0.40	0.68	13.10	0.62	Failure
5	1.0125	1.20	0.81	25.03	0.76	Failure
4	1.0100	2.73	0.97	55.10	1.30	Failure
3	1.0075	7.63	1.06	233.50	1.67	Failure
2	1.0050	22.93	1.48	1,673.67	2.00	Failure
1	1.0025	217.27	1.63	8,357.00	2.20	Failure
1	1.0000	117.23	1.08	2,840.33	1.08	No failure
1	0.9500	111.03	0.83	2,531.33	0.79	No failure
1	0.9000	117.23	0.51	2,851.67	0.48	No failure

Table 4 Summary of residual-state creep tests on mica-rich sample

Test	RCSR	T_1 (min)	D_1 (mm)	T_2 (min)	D_2 (mm)	Remarks
7	1.0200	0.37	1.53	1.20	0.67	Failure
6	1.0150	0.60	0.56	3.17	0.82	Failure
5	1.0125	1.10	0.60	5.50	0.94	Failure
4	1.0100	4.33	1.23	23.17	1.50	Failure
3	1.0075	9.50	1.39	51.00	2.22	Failure
2	1.0050	40.03	1.95	219.57	2.40	Failure
1	1.0025	914.00	0.54	5,013.07	2.44	Failure
1	1.0000	140.67	0.95	3,198.83	0.95	No failure
1	0.9500	133.17	0.65	3,036.80	0.65	No failure
1	0.9000	114.00	0.59	2,724.67	0.59	No failure

Table 5 Summary of residual-state creep tests on chlorite-rich sample

Test	RCSR	T_1 (min)	D_1 (mm)	T_2 (min)	D_2 (mm)	Remarks
7	1.0200	0.30	0.70	0.70	1.20	Failure
6	1.0150	0.47	1.07	1.83	1.39	Failure
5	1.0125	0.97	1.36	3.17	1.51	Failure
4	1.0100	4.17	1.76	13.37	2.07	Failure
3	1.0075	9.23	2.56	29.30	2.79	Failure
2	1.0050	32.73	2.59	125.47	2.97	Failure
1	1.0025	950.33	2.9	2,848.33	2.99	Failure
1	1.0000	123.30	1.89	4,324.00	1.89	No failure
1	0.9500	114.17	1.81	4,250.83	1.81	No failure
1	0.9000	115.83	1.37	3,848.00	1.37	No failure

Table 6 Summary of residual-state creep tests on smectite-rich sample

Test	RCSR	T_1 (min)	D_1 (mm)	T_2 (min)	D_2 (mm)	Remarks
7	1.0200	0.17	0.90	0.37	1.50	Failure
6	1.0150	0.27	1.37	0.97	1.80	Failure
5	1.0125	0.53	1.60	1.67	2.21	Failure
4	1.0100	2.40	1.96	5.37	3.04	Failure
3	1.0075	5.30	2.65	15.43	3.61	Failure
2	1.0050	18.70	2.61	66.03	4.08	Failure
1	1.0025	543.07	2.98	1,499.13	4.15	Failure
1	1.0000	100.90	2.36	3,459.20	2.36	No failure
1	0.9500	95.00	2.17	3,541.67	2.17	No failure
1	0.9000	90.33	1.86	3,075.33	1.86	No failure

strength. Based on the concepts of Lefebvre (1981), Leroueil (1998) and Hunter and Khalili (2000) proposed that the creeping displacement behavior may be initiated from the fully softened (or critical state). Every soil is considered first to have a zone of creep just below the strength envelope, with a lower boundary equivalent to 90–95 % of the angle of shearing resistance (Ter-Stepanian 1963; Yen 1969). But this study shows that the creeping displacement behavior is initiated from the residual-state of shear and there is no significant creeping effect on and below the residual-state of shear (Tables 3, 4, 5, 6). That means when RCSR ≤1, the soil does not show creeping displacement behavior, and the soil undergoes creeping displacement behavior when RCSR >1. The mechanism behind it may be that the coefficient of static friction (μ_s) is working in primary and secondary stages of creep, but in the case of tertiary creep, the coefficient of dynamic friction (μ_k) may work. We know that the coefficient of static friction (μ_s) is always greater than the coefficient of dynamic friction (μ_k) (i.e., $\mu_s > \mu_k$). That means the stage of creep where μ_s is effective can resist the applied creep load rather than the zone of creep where μ_k is effective. When RCSR ≤1, the force between the soil particles is influence by μ_s, which keeps the specimen in stable condition. Similarly, when RCSR >1, the force between the soil particles is influenced by μ_k, which may leading to failure. However, the reason why and how the coefficient of static friction and dynamic friction are effective in different stages of creep needs further investigation.

The nature of the curve in primary stage of creep consists of logarithmic curves, secondary stage of creep shows linear, and parabolic in tertiary creep (Figs. 6, 7, 8, 9). In primary creep, the smectite-rich sample shows the smooth curve nature, and chlorite-rich sample and mica-rich sample followed it, respectively (Figs. 7, 8, 9). The mica-rich sample showed the steep curve nature in the stage of tertiary creep (Fig. 7). The nature of secondary creep for all tested samples was almost a similar pattern; however, the smectite-rich sample and the chlorite-rich sample showed slightly steeper slopes than the mica-rich sample. In tertiary creep, the smectite-rich sample showed a smooth parabolic curve with a higher radius of curvature, and the chlorite-rich sample and the mica-rich sample followed it, respectively (Figs. 7, 8, 9). The smectite-rich sample and the chlorite-rich sample showed tertiary creeping behavior over long periods of time, with maximum displacement comparable to the mica-rich sample before leading to failure (Tables 3, 4, 5, 6), which means the range of tertiary creep in the smectite-rich sample and the chlorite- rich sample was higher than mica-rich sample and kaolin clay.

Based on the time periods upon primary creep, secondary creep, and tertiary creep (Tables 3, 4, 5, 6), the creeping zone was evaluated. Figures 10, 11, 12, and 13 show the evaluation for the creep zone of kaolin clay, mica-rich sample, chlorite-rich sample, and smectite-rich sample, respectively. The blue enclosed area shows the primary creep zone, where the specimen is stable. The red enclosed areas indicated the tertiary creep zone, where test specimen is reached to fail (Figs. 10, 11, 12, 13). In case of the kaolin clay and the mica-rich sample, the range of secondary creep was wider, but the smectite-rich sample and the chlorite-rich sample show the wider range of tertiary creep (Figs. 10, 11, 12, 13). This means that the kaolin clay and the mica-rich samples are stable in long time with compare to the smectite-rich sample and the chlorite-rich sample. The ring shear test results show that the peak strength and the residual strength of the kaolin clay are higher, followed by mica-rich sample, chlorite-rich sample, and smectite-rich sample, respectively (Fig. 5). However, the difference between the peak strength and the residual strength of the kaolin clay is lower, and mica-rich sample, chlorite-rich sample, and smectite-rich sample followed it, respectively. It was observed that the kaolin clay is the strongest and the smectite-rich sample is the weakest. The smectite-rich sample and the chlorite-rich sample show the high plasticity in the soil's nature. Similarly, the kaolin clay shows low plasticity in its soil nature. This means that the kaolin clay and the mica-rich samples are stable over a long time compared with the smectite-rich sample and the chlorite-rich sample. High
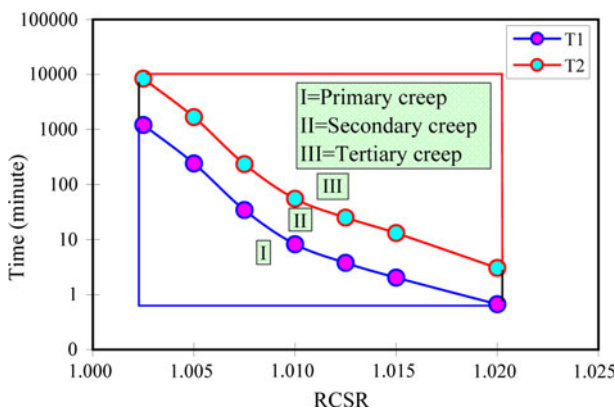

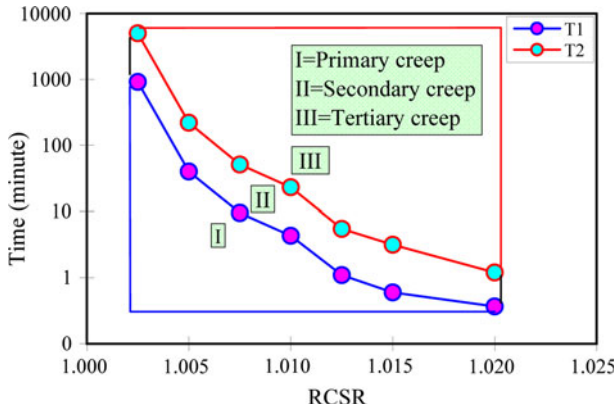**Fig. 10** Evaluation of creep zone on kaolin clay

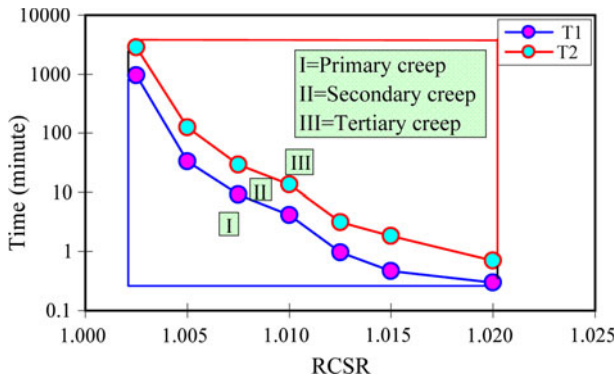**Fig. 11** Evaluation of creep zone on mica-rich sample

Fig. 12 Evaluation of creep zone on chlorite-rich sample
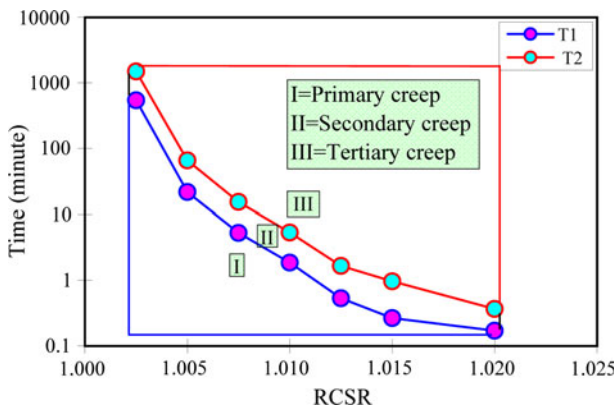

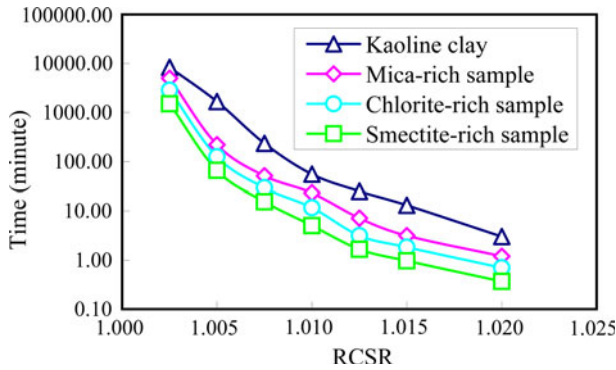**Fig. 13** Evaluation of creep zone on smectite-rich sample

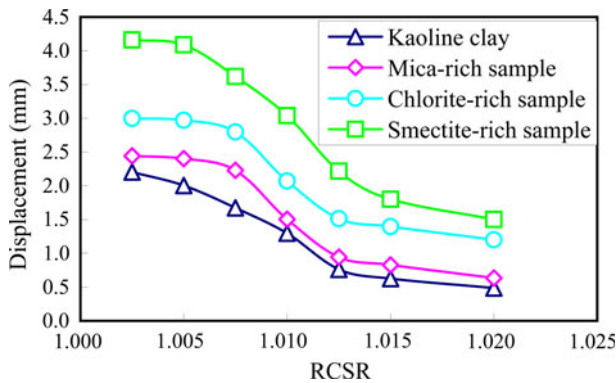**Fig. 14** Prediction curves (Time vs. RCSR)

Fig. 15 Prediction curves (Displacement vs. RCSR)

plasticity soils, which have large drop from peak strength to residual strength, have a higher chance to reach the tertiary creep zone in short time compared with the low plasticity soils.

The prediction curves (Time vs. RCSR) based on the tertiary creep results are presented in Fig. 14. This curve can be predicted as the time to complete failure (min) with corresponding to RCSR value. For example, if RCSR is 1.0025, the smectite-rich sample will reach failure after 1,499.13 min, but in the case of the chlorite-rich sample, test specimens resist the applied constant creep load up to 2,848.33 min. Similarly, the mica-rich sample and the kaolin clay began tertiary creep after 5,013.07 and 8,357.00 min, respectively (Fig. 14). Failure trends show that the smectite-rich sample failed in less time with respect to other tested specimens. The ranges of failure time with varying RCSR, 1.0025–1.0200, are 1,499.13–0.37 min, 2,848.33–0.70 min, 5,013.07–1.20 min, and 8,357.00–3.03 min on smectite-rich sample, chlorite-rich sample, mica-rich sample, and kaolin clay, respectively (Tables 3, 4, 5, 6). Test results show that clay from landslide soil, which has minimum residual-state of shear, shows significant creeping displacement behavior. Hence, the smectite-rich sample failed in a short time; then, chlorite-rich sample, mica-rich sample, and kaolin clay failed, respectively (Fig. 14). Similarly, the prediction curve (Displacement to RCSR) was proposed based on test results, as shown in Fig. 15. In this prediction curve, the smectite-rich sample had maximum displacement before failure and chlorite-

rich sample, mica-rich sample, and kaolin clay followed it, respectively (Fig. 15). Results show that the presence of a greater composition of weak clayey minerals such as smectite and chlorite indicates a significant role in reactivation and creeping displacement behavior.

4 Conclusions

Landslides are one of the major natural disasters in mountainous regions. A large amount of the budget is spent managing these landslides. The major interest in these landslides continues to be minimizing the creeping displacement of these landslides and thereby reducing the damage risk to the human settlement, structures, and environment over the landslides' mass. However, the creeping displacement behavior of such landslides and associated issues are not fully understood, especially in relation to the displacement behavior of the residual-state of shear of the slip surface clayey soil. This paper has primarily addressed this issue with the help of experimental results of typical clayey soils and has attempted to interpret the results toward the possibilities of predicting landslide displacement.

A residual-state creep test apparatus was developed, which is capable of measuring creep displacement with respect to time under the application of a constant creep stress. A concept of the residual-state creep test and its testing procedures was developed to understand the creep displacement behavior of clayey soils. The ideal creep curve for a soil material was verified in the test procedure and was found to perfectly matching with obtained results. The test results on four typical clayey soils show that the creep failure begins only when the applied shear stress (i.e., creep stress) is above the residual strength and that there is no creeping effect on or below the residual strength. The prediction curves of creep failure trend show that the smectite-rich sample failed in a short time compared with other samples while the displacement until the failure was found to be large. These results indicate that the presence of weaker clayey minerals, such as smectite and chlorite, significantly influences the reactivation of a landslide and its creep displacement behavior. Residual-state creep failure prediction curves are proposed as the major output of this study, which may be used to predict failure time and displacement of creeping landslides in the future.

References

Andersland OB, Akili W (1967) Stress effect on creep rates of a frozen clay soil. Geotechnique 17(1):27–39
Augustesen A, Liingaard M, Lade PV (2004) Evaluation of time dependent behavior of soils. Int J Geomech 4(3):137–156

Bhat DR, Bhandari NP, Yatabe R, Tiwari RC (2011a) Residual-state creep test in modified torsional ring shear machine: methods and implications. Int J GEOMATE 1(1):39–43

Bhat DR, Bhandari NP, Yatabe R, Tiwari RC (2011b) Prediction of large-scale landslide based on tertiary creep test by modified ring shear apparatus. In: Proceedings of the thirteenth international summer symposium, Japan, pp 179–182

Bhat DR, Bhandari NP, Yatabe R, Tiwari RC (2011c) Method of residual-state creep test using Torsional ring shear machine. In: Proceedings of 46th National convention of Japanese Geotechnical Society, Japan, pp 928–929

Bhat DR, Bhandari NP, Yatabe R, Tiwari RC (2011d) Pre-peak and post-peak creep test using torsional ring shear machine. In: Proceedings of Annual Convention of Japan Society of Civil Engineers (JSCE), Japan, III-374, pp 747–748

Bhat DR, Bhandari NP, Yatabe R, Tiwari RC (2012a) A new concept of Residual-State Creep Test to understand the creeping behavior of clayey soils. Geotech Spec Publ ASCE 225:683–692. doi:10.1061/9780784412121.071

Bhat DR, Bhandari NP, Yatabe R, Tiwari RC (2012b) Creep behavior of clayey soils in residual-state of shear: an experimental study to understand the creeping displacement behavior of large-scale landslides. In: Proceedings of the 11th international and 2nd North American symposium on landslides, Banff, Alberta, Canada, pp 995–1000

Bishop AW, Green GE, Garge VK, Andersen A, Brown JD (1971) A new ring shear apparatus and its application to the measurement of residual strength. Geotechnique 21(4):273–328

Bonzanigo L, Eberhardt E, Loew S (2007a) Long-term investigation of deep seated creeping landslide in crystalline rock. Part I. Geological and hydro mechanical factors controlling the Campo Vallemaggia landslide. Can Geotech J 44:1157–1180

Bonzanigo L, Eberhardt E, Loew S (2007b) Long-term investigation of deep seated creeping landslide in crystalline rock. Part II. Mitigation measure and numerical modeling of deep drainage at Campo Vallemaggia landslide. Can Geotech J 44:1181–1199

Brandes HG, Nakayama DD (2010) Creep, strength and other characteristics of Hawaiian volcanic soils. Geotechnique 60(4):235–245

Bromhead EN (1979) A simple ring shear apparatus. Ground Eng 12(5):40–44

Bromhead EN, Curtis RD (1983) A comparison of alternative methods of measuring the residual strength of London clay. J Ground Eng 16(4):39–40

Bromhead EN, Dixon N (1986) The field residual strength of London clay and its correlation with laboratory measurements, especially ring shear tests. Geotechnique 36(3):449–452

Campanella RG, Vaid YP (1974) Triaxial and plane strain creep rupture of an undisturbed clay. Can Geotech J 11(1):1–10

Chandler RJ (1977) Back analysis techniques for slope stabilization works: a case record. Geotechnique 27(4):479–495

Eberhardt E, Bonzanizo L, Loew S (2007a) Long-term investigation of deep seated creeping landslide in crystalline rock. Part I Geological and hydro mechanical factors controlling the Campo Vallemaggia landslide. Can Geotech J 44:1157–1180

Eberhardt E, Bonzanizo L, Loew S (2007b) Long-term investigation of deep seated creeping landslide in crystalline rock. Part II Mitigation measure and numerical modeling of deep drainage at Campo Vallemaggia landslide. Can Geotech J 44:1181–1199

Feda J (1989) Interpretation of creep of soil by rate process theory. Geotechnique 39(4):667–677

Gibo S (1994) Ring shear apparatus in measuring residual strength and its measurement accuracy. J Jpn Landslide Soc 31(3):24–30 (in Japanese with English abstract)

Gibo S, Egashira K (1992) Relation between reorientation of clay particles and the residual strength of mudstone of the Shimajiri group. Trans Jpn Soc Irrig Drain Reclam Eng 161:19–24 (in Japanese with English abstract)

Hunter G, Khalili N (2000) A simple criterion for creep induced failure of over-consolidated clays. In: Proceedings of Geo Eng Conference, Melbourne, Australia (CD format, Paper ID: IS-2000-474)

La Gatta DP (1970) Residual strength of clays and clay-shales by rotation shear tests. PhD thesis reprinted as Harvard Soil Mechanics Series, No 86, Harvard University, Cambridge, USA, p 204

Lefebvre G (1981) Fourth Canadian Geotechnical Colloquium: strength and slope stability in Canadian soft clay deposits. Can Geotech J 18:420–422

Leoni M, Karstunen M, Vermeer PA (2008) Anisotropic creep model for soft soils. Geotechnique 58(3):215–226

Leroueil S (1998) Elements of time-dependent mechanical behaviour of overconsolidated clays. In: Proceedings of 51st Canadian Geotechnical Conf, Edmonton, vol 2, pp 671–677

Leroueil S, Kabbaj M, Tavenas F, Bouchard R (1985) Stress–strain–strain rate relation for the compressibility of sensitive natural clays. Geotechnique 35(2):159–180

Lupini JF, Skinner AE, Vaughan PR (1981) The drained residual strength of cohesive soils. Geotechnique 31(2):181–213

Meehan CL, Brandon TL, Duncan JM, Tiwari B (2010) Direct shear testing of polished slickensided surfaces. Landslides 7(2):157–167

Mesri G, Feng TW (1986) Discussion, Stress–strain rate relation for the compressibility of sensitive natural clays by S Leroueil et al. Geotechnique 36(2):283–290

Mesri G, Shahien M (2003) Residual shear strength mobilized in first-time slope failures. J Geotech Geoenviron Eng ASCE 129(1):12–31

Morgenstern NP Tchalenko JS (1967) Microstructural characteristics on shear zones from slips in natural clays. In: Proceedings of geotechnical conference, Uslo, vol 1, pp 147–152

Nakamura S, Gibo S, Egashira K, Kimura S (2010) Platy layer silicate minerals for controlling residual strength in landslide soils of different origins and geology. Geology 38(8):743–746

Patton FD (1984) Climate, groundwater pressures and stability analyses of landslides. In: Proceedings of the IVth international symposium on landslides, vol 3, pp 43–60

Picarelli L, Urciuoli G, Russo C (2001) Effect of groundwater regime on the behavior of clayey slopes. Can Geotech J 41:1995–2004

Picarelli L, Urciuoli G, Russo C (2004) The role of groundwater regime on behavior of clayey slopes. Can Geotech J 41:467–484

Sassa K (1992) Access to the dynamics of landslides during earthquakes by a new cyclic loading ring shear apparatus. In: Proceedings of the 6th international symposium on landslides, Balkema, Rotterdam, vol 3, pp 1919–1937

Skempton AW (1964a) Long-term stability of clay slopes. Geotechnique 14(2):75–101

Skempton AW (1964b) Fourth rankine Lecture: long term stability of clay slope. Geotechnique 14(2):75–102

Skempton AW (1970) First time slides in over consolidated clays. Geotechnique 20(3):320–324

Skempton AW (1985) Residual strength of clays in landslides, folded strata and the laboratory. Geotechnique 35(1):3–18

Skempton AW, Petley DJ (1967) The strength along structural discontinuities in stiff clays. In: Proceedings of geotechnical conference, Oslo, Norway, vol 2, pp 29–47

Stark T, Eid H (1994) Drained residual strength of cohesive soils. J Geotech Geoenviron Eng, ASCE 120(5):856–871

Stark T, Choi H, McCone S (2005) Drained shear strength parameters for analysis of landslides. J Geotech Geoenviron Eng ASCE 131(5):575–588

Suklje L (1969) Rheological aspects of soil mechanics. Wiley-Interscience, London. Found Div SM 4:1075–1096

Suzuki M, Tsuzuki S, Yamamoto T (2007) Residual strength characteristics of naturally and artificially cemented clays in reversal direct box shear test. Soils Found 47(6):1029–1044

Ter-Stepanian G (1963) On the long term stability of slopes. Nor Geotech Inst 52:1–14

Ter-Stepanian G (1975) Creep of a clay during shear and its rheological model. Geotechnique 25(2):299–320

Terzaghi K (1950) Mechanism of landslide, In application of Geology to Engineering Practice, Berkey Volume, Geological Society of America, pp 83–123

Nelson JD, Thompson, EG (1977) A theory of Creep Failure in over consolidated Clay. In: Journal of the Geotechnical Engineering, Proceedings of the American Society of Civil Engineers, 103(11), pp 1281–1293

Tika TE (1999) Ring shear tests on a carbonate sandy soil. Geotech Test J 22(4):342–355

Tika TE, Hutchinson JN (1999) Ring shear tests on soil from the Vaiont landslide surface. Geotechnique 49(1):59–74

Tiwari B, Marui H (2005) A new method for the correlation of residual shear strength of the soil with mineralogical composition. J Geotech Geoenviron Eng ASCE 131(9):1139–1150

Tori T, Kitagawa R (2006) Mineralogical characteristics of smectite formed in the toyooka tuff formation of the kobe group-special attention to the occurrence of landslide in this region. Clay Sci Soc Jpn 45(4):238–249 (in Japanese with English abstract)

Waker LK (1969) Undrained creep in sensitive clay. Geotechnique 19(4):515–529

Wan Y, Kwong J (2002) Shear strength of soils containing amorphous clay-size materials in a slow-moving landslide. Eng Geol 65:293–303

Yatabe R, Yagi N, Enoki M, Nakamori K (1991) Strength characteristics of landslide clay. J Jpn Landslide Soc 28(1):9–16 (in Japanese with English abstract)

Yatabe R, Bhandary N, Okamura M (2007) Geotechnical perspectives of landslide mechanism in serpentine zone. Clay Sci Soc Jpn 46(1):16–23 (in Japanese with English abstract)

Yen BC (1969) Stability of slopes undergoing creep deformation. Soil Mech Found Div SM 4:1075–1096

Yin ZY, Chang CS, Karstunen M, Hicher PY (2010) An anisotropic elastic–viscoplastic model for soft clays. Int J Sol Struct 47:665–677